

1. INTRODUCTION

A crucial issue to analyse the induced seismicity for hydraulic fracturing is the detection and location of near signals so-called acoustic emissions (AE) activity with robust and sufficiently accurate automated algorithms. Waveform stacking and coherence techniques are here adapted to detect and locate AE signals for massive datasets with extremely high sampling rate (1 MHz). These techniques are applied for the first time using a full waveform approach for a hydraulic fracturing experiment (Nova project 54-14-1) that took place 410 m below surface at the Äspö Hard Rock Laboratory, Sweden (Figure 1a). Zang et al. (2017) described the overall goal of the experiment and provided a reference catalogue of AE hypocentres obtained from four hydraulic fractures based on the in situ trigger recording. We present the results obtained during the conventional, continuous water-injection experiment Hydraulic Fracture 2 (HF2) using continuous waveform recording from 11 AE sensors with highest sensitivity in the frequency range 1 to 100 kHz (Figure 1b). Hydraulic testing horizontal borehole was drilled to a total length of 28.40 meter. HF2 is located at 22.5 m borehole length and recorded the most significant seismicity with 102 AE events relocated in the in situ triggered reference catalogue.

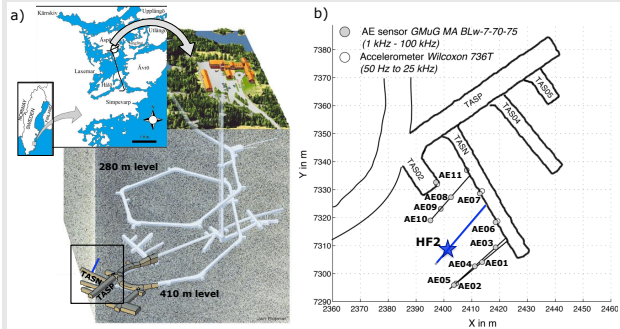


Figure 1. a) Test site for hydraulic fracturing in an experimental tunnel of Äspö Hard Rock Laboratory (Sweden). b) Sensors are employed in the near-field; a blue line indicates the hydraulic testing borehole, the blue star identifies the fluid injection segment corresponding to the HF2 experiment.

2. FULL WAVEFORM DETECTION AND AUTOMATED LOCATIONS USING COHERENCE

We consider continuous recordings and apply a recently developed automated full waveform detection, which relies on the stacking of characteristic functions (python-based earthquake detector so-called "Lassie", Heimann et al., 2017). It follows a delay-and-stack approach, where the likelihood of the hypocenter location in a pre-selected seismicogenic volume is mapped by assessing the coherence of the P onset times at different stations. The resulting catalogue is composed of 4158 AEs (Figure 2). The inspection of the temporal evolution of signal detection reveals that 85% of AEs take place during the phases of increased flow rate and increasing pressure, dropping very quickly in time as soon as the pressure decrease and the flow stopped. The location of the AE events is refined using an accurate waveform stacking and coherence method which uses both P and S phases (Figure 3). Moreover, the relative location accuracy can be improved using a master event approach (Grigoli et al. 2016).

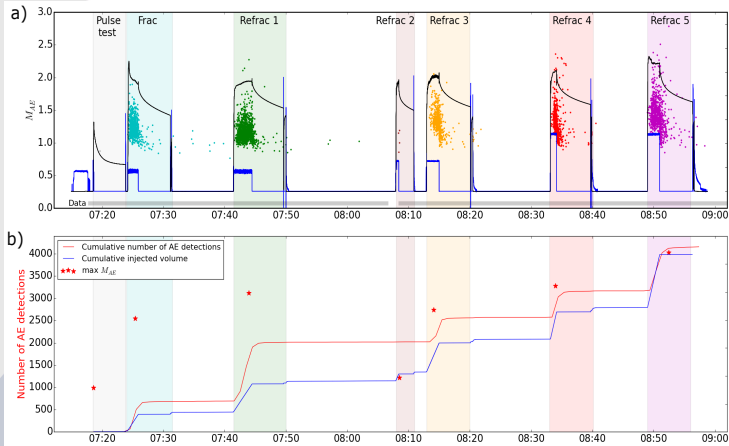


Figure 2. a) Distribution of the AE events according to the AE magnitude (M_{AE}) for the whole HF2 experiment. AE events are identified for different colors according the different stages for HF2: Pulse Test, initial fracture phase (Frac) and the propagation of the rupture during different refracturing (Refrac 1 - 5). b) Comparison between cumulative number of AE events and injected volume. The maximum M_{AE} (red stars) and a bar diagram for the number of AE events (figure inset) is also shown for each stage.

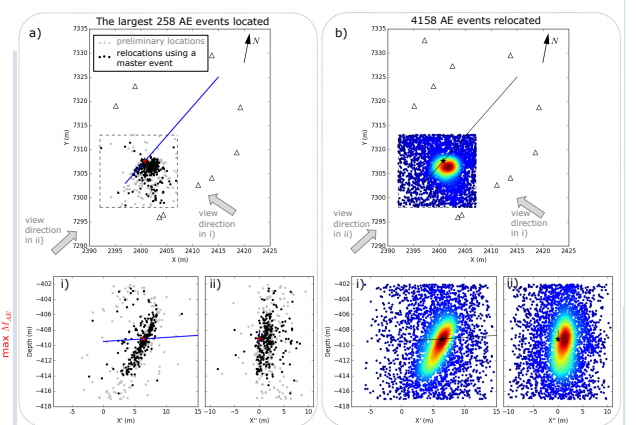


Figure 3. a) Small subset of the largest AE events are located with two techniques: waveform coherence analysis (gray dots) and relocation using a master event (black dots). b) All AE events relocated using a master event (4158 AEs) showing the Gaussian Kernel density where red denotes higher density and blue regions with few events. A 3D grid is generated around the hydraulic fracturing volume (15 x 15 x 15 m) using a size grid of 10 cm.

3. FREQUENCY-MAGNITUDE DISTRIBUTION

We estimate the AE magnitudes (M_{AE}) to evaluate the frequency-magnitude distribution obtaining a high b-value of 2.38 (Figure 4). The magnitude of completeness is also estimated around M_{AE} 1.1 and we observe an interval range of M_{AE} between 0.77 and 2.79.

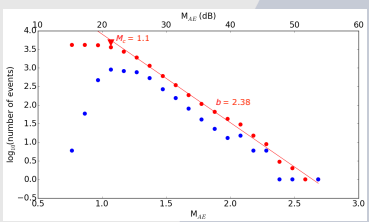


Figure 4. Frequency-magnitude distribution (FMD) of the overall catalogue for the HF2 experiment. Red line shows the best fit for the cumulative FMD (red dots). Non-cumulative FMD is also shown with blue dots.

5. DISCUSSION & CONCLUSIONS

- Robust and sufficiently accurate AE locations are reached applying waveform stacking and coherence analysis. Triggered based approach (Zang et al., 2017) was able to detect 102 events in the same dataset, whereas our catalogue is more than 40 times larger (4158 events).
- High b-value (2.38) and the magnitude of completeness (M_{AE} 1.1) are obtained for the HF2 experiment.
- The maximum observed magnitude increases with time in the fracturing experiment reaching its maximum value (M_{AE} , max 2.79) at the end of the experiment (Refrac 5) when the injected volume is largest.
- Preliminary results from the in situ trigger mode (Zang et al., 2017) are compatible with our interpretations. However, thanks to the implementation of these novel techniques, we are able to support our finding on a much broader catalogue (more information in López-Comino et al., 2017).

4. THE FRACTURE GROWTH

The hydraulic fractures growth is then characterized by mapping the spatiotemporal evolution of AE hypocentres. The microseismicity is spatially clustered in a prolate ellipsoid, resembling the main fracture volume ($\sim 105 \text{ m}^3$), where the length of the principal axes ($a = 10 \text{ m}$; $b = 5 \text{ m}$; $c = 4 \text{ m}$) define its size and its orientation can be estimated for a rupture plane (strike $\sim 123^\circ$, dip $\sim 60^\circ$) (Figure 5 and 6). An asymmetric rupture regarding to the fracturing borehole is clearly exhibited. AE events migrate upwards covering the depth interval between 404 and 414 m. After completing each injection and reinjection phase, the AE activity decreases and appears located in the same area of the initial fracture phase, suggesting a crack-closing effect.

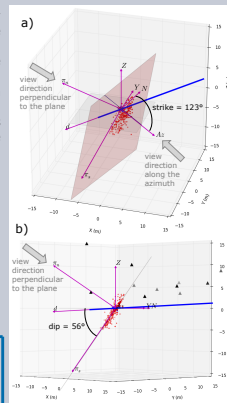


Figure 5. 3D views for the main rupture plane (red plane) that is defined considering the locations of the largest AE events ($M_{AE} > 1.5$) inside the cluster volume (red dots) from the figure 3b: a) perspective view and b) side view along the azimuth of the rupture plane.

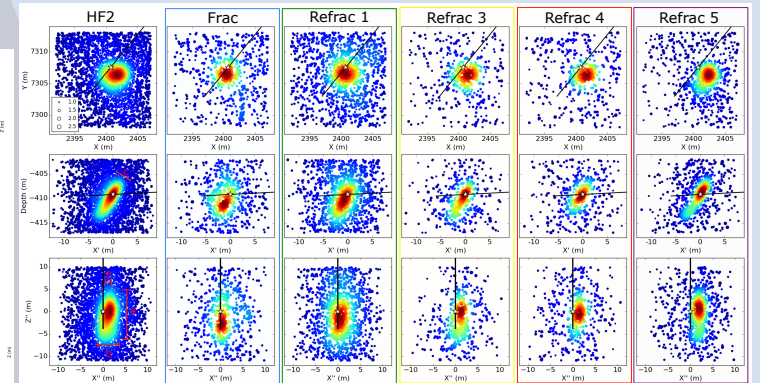


Figure 6. The fracture growth is analyzed from the locations of the AE events showing the Gaussian Kernel density where red denotes a higher density of AE sources and blue regions with few events. Results are shown according the different stages for HF2. Dots are scaled according the M_{AE} (see legend in the first box). Three perspective views are shown: view from above (first row), side view along the azimuth of the rupture plane (second row) and side view perpendicular to the rupture plane (third row).

REFERENCES

Zang A., O. Stephansson, L. Stenberg, K. Plenkens, C. Milkereit, G. Kwiatek, G. Dresen, E. Schill, G. Zimmermann, T. Dahm and M. Weber (2017). Hydraulic fracture monitoring in hard rock at 410 m depth with an advanced fluid-injection protocol and extensive sensor array. *Geophysics*, J. Int., 208, 2, p. 790-813.
 Heimann S., C. Matos, S. Cesca, I. Rio and S. Custodio (2017). Lassie: A versatile tool to detect and locate seismic activity, *Seismological Research Letters*, in preparation. Note: interested users to preview Lassie can write to: sebastian.heimann@gfz-potsdam.de
 Grigoli, F., S. Cesca, L. Krieger, M. Kriegerowski, S. Gammali, J. Horalek, E. Priolo, T. Dahm (2016). Automated microseismic event location using Master-Event Waveform Stacking, *Scientific Reports*, 6, 25744, doi: 10.1038/srep25744
 López-Comino, J. A., S. Cesca, S. Heimann, F. Grigoli, C. Milkereit, T. Dahm and A. Zang (2017). Characterization of hydraulic fractures growth during the Äspö Hard Rock Laboratory experiment (Sweden). *Journal of Rock Mechanics and Rock Engineering*, under review